

Article

A Zn(II)–Metal–Organic Framework Based on 4-(4-Carboxy Phenoxy) Phthalate Acid as Luminescent Sensor for Detection of Acetone and Tetracycline

Nairong Wang, Shanshan Li, Zhenhua Li, Yuanyuan Gong and Xia Li *

Department of Chemistry, Capital Normal University, Beijing 100048, China

* Correspondence: xiali@cnu.edu.cn

Abstract: As hazardous environmental pollutants, residual tetracycline (TC) and acetone are harmful to the ecosystem. Therefore, it is necessary to detect the presence of these pollutants in the environment. In this work, using Zn (II) salt, 4-(4-carboxy phenoxy) phthalic acid (H_3L), and 3,5-bis(1-imidazolyl) pyridine (BMP), a new metal–organic framework (Zn-MOF) known as $[Zn_3(BMP)_2L_2(H_2O)_4] \cdot 2H_2O$ was synthesized using a one-pot hydrothermal method. The Zn-MOF has a three-dimensional framework based on the $[Zn_1N_2O_2]$ and $[Zn_2N_2O_4]$ nodes linked by a tridentate bridge BMP ligand and an L ligand with the $\mu_1\text{-}\eta^1\eta^0 / \mu_1\text{-}\eta^1\eta^0 / \mu_0\text{-}\eta^0\eta^0$ coordination mode. There were two kinds of left- and right-handed helix chains, Zn1-BMP and Zn1-BMP-Zn1-L. The complex was stable in aqueous solutions with pH values of 4–10. The Zn-MOF exhibited a strong emission band centered at 385 nm owing to the $\pi^* \rightarrow \pi$ electron transition of the ligand. It showed high luminescence in some common organic solvents as well as in the aqueous solutions of pH 4–10. Interestingly, TC and acetone effectively quenched the luminescence of the Zn-MOF in aqueous solution and enabled the Zn-MOF to be used as a sensor to detect TC and acetone. The detection limits of TC and acetone were observed to be 3.34 μM and 0.1597%, respectively. Even in acidic (pH = 4) and alkaline (pH = 10) conditions, the Zn-MOF showed a stable luminescence sensing capability to detect TC. Luminescence sensing of the Zn-MOF for TC in urine and aquaculture wastewater systems was not affected by the interfering agent. Furthermore, the mechanism of sensing TC was investigated in this study. Fluorescence resonance energy transfer and photoinduced electron transfer were found to be the possible quenching mechanisms via UV–Vis absorption spectra/the excitation spectra measurements and DFT calculations.

Keywords: luminescent sensor; tetracycline; acetone; metal–organic framework

Citation: Wang, N.; Li, S.; Li, Z.; Gong, Y.; Li, X. A Zn(II)–Metal–Organic Framework Based on 4-(4-Carboxy Phenoxy) Phthalate Acid as Luminescent Sensor for Detection of Acetone and Tetracycline. *Molecules* **2023**, *28*, 999. <https://doi.org/10.3390/molecules28030999>

Academic Editor: Peizhou Li

Received: 30 December 2022

Revised: 14 January 2023

Accepted: 17 January 2023

Published: 19 January 2023



Copyright: © 2023 by the authors. Licensee MDPI, Basel, Switzerland. This article is an open access article distributed under the terms and conditions of the Creative Commons Attribution (CC BY) license (<https://creativecommons.org/licenses/by/4.0/>).

1. Introduction

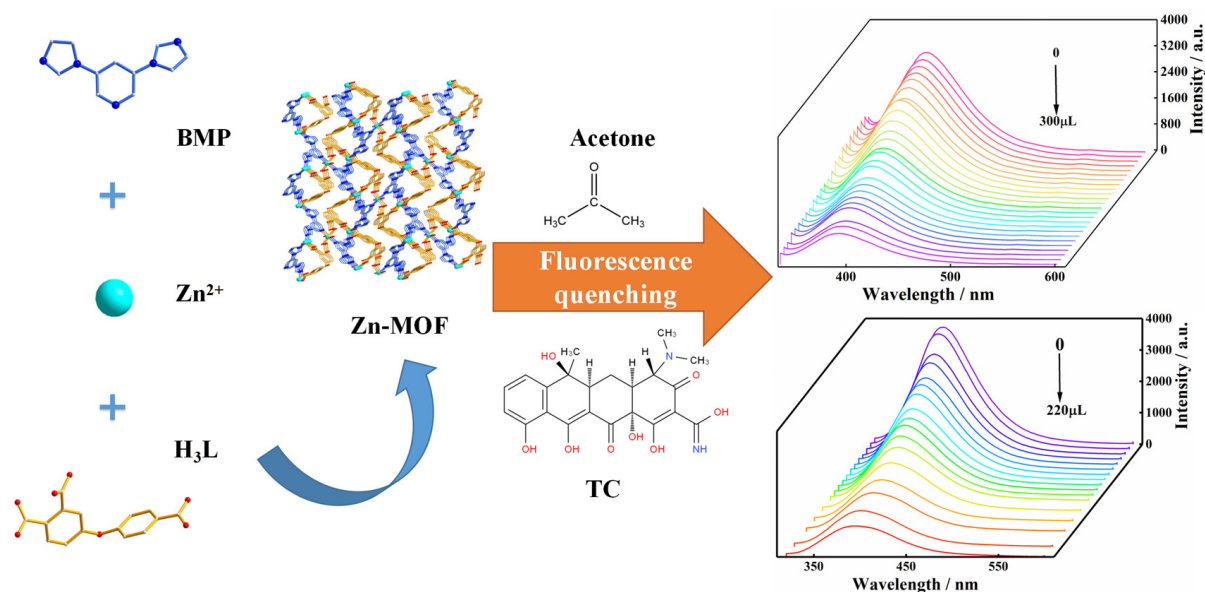
Environmental pollutants easily spread into the soil, air, and water environments due to their high solubility and mobility. The high prevalence of these pollutants in the ecosystems is gravely threatening the environment and human health and has become a global concern [1]. The massive use of antibiotics and pesticides has led to the emergence of super-resistant bacteria [2]. Residual solvent molecules in the environment can also cause cancer, malformation, neurotoxicity, and other health problems [3]. Belonging to the class of broad-spectrum antibiotics, tetracycline (TC) is widely used in treating human and animal bacterial infections due to its low toxicity, low cost, and excellent oral absorption. However, TC is not fully absorbed during animal metabolism and enters the environment with feces. Hence, large amounts of TC residues are often found in soil and water environments [4–6]. In addition, acetone is a typical volatile organic solvent widely used in cosmetics, adhesives, and other commercial products. Long-term exposure to acetone may damage the liver, kidneys, and nerves, causing inflammation [7–9]. Acetone is readily found in industrial wastewater environments. Currently, high-performance liquid chromatography (HPLC), capillary electrophoresis (CE), and immunoassay are common

methods for detecting environmental pollutants such as tetracycline and acetone [10–12]. However, these methods generally require expensive and sophisticated instruments, complex pre-processing procedures, and skilled technicians, which are not conducive to rapid and routine monitoring [13–16]. Therefore, it is crucial to develop a fast and simple method for detecting TC and acetone.

Metal–organic frameworks (MOFs), a group of porous materials composed of inorganic metal ions and organic bridging ligands, have sparked a lot of academic interest in recent years [17–19]. MOFs have flexible structural designs, highlighting a specific surface area and highly ordered pores. Therefore, MOFs have been widely explored for the storage and separation of various gases as well as catalytic [20–23], biomedical [24], magnetic [25,26], and chemical sensing applications [27–29]. Luminescent metal–organic frameworks, as an important family of MOF materials, have made outstanding contributions in detecting harmful pollutants such as antibiotics, solvent molecules, pesticides, explosives, and other pollutants due to their superior luminescence ability [30–34]. In recent years, MOFs have also made positive advances in detecting tetracycline and acetone. Huang et al. synthesized an Fe-modified MXene-derived MOF that can be used as a high-performance acetone sensor [35]. Gan et al. proposed fluorescent Eu-MOF designed to detect TC rapidly in food samples [36]. Zn(II) ion with d^{10} electronic configuration possesses not only various coordination modes but also attractive luminescence properties when bound to functional ligands. Due to these characteristics, the Zn-MOFs have been reported as sensors for detecting antibiotics, metal ions, and small molecules [37–39]. For example, $\{[Zn(L)_{0.5}(bpea)] \cdot 0.5H_2O \cdot 0.5DMF\}_n$ has been reported to be an effective luminescence sensor for nitrofurazone (NFT) in aqueous solutions with an LOD of $0.35 \mu M$ [40]. $[Zn_2(tdca)_2(bppd)_2] \cdot 2DMF$ can be used as a sensitive luminescence probe for the detection of Cd^{2+} [41].

In general, the preparation of luminescent MOFs requires the selection of ligands with luminescence properties and functional groups with the ability to modify the luminescence properties, in addition to different photoactive metal ions [15]. The luminescence properties of MOFs can be adjusted by introducing organic ligands with aromatic groups or conjugated π -systems through conjugation effects [42]. Due to their strong coordination, aromatic carboxylic acid ligands are the best candidates to form MOFs. 4-(4-carboxy phenoxy) phthalic acid (H_3L) is a V-type semi-rigid carboxylic acid. The two benzene rings of the ligands can rotate through ether groups and exhibit some conformational flexibility [43]. In addition, it contains three carboxylic acid groups, with the metal center in different ligand coordination ways. It makes the formation of MOFs easy to obtain and with great structural diversity. It has been reported that a series of Zn(II) complexes constructed by the H_3L ligand have 3D frameworks and good luminescence properties, which provide the possibility for the synthesis of the luminescent Zn-MOF [44]. The introduction of N-containing heterocyclic organic ligands can enrich the design of the complex. 3,5-bis(1-imidazolyl) pyridine (BMP) is a rigid nitrogenous heterocyclic ligand with large conjugated groups that readily form coordination bonds with metals and increase the stability of the structure [45,46].

Here, in this work, the H_3L ligand and BMP ligand were used to synthesize new MOFs by employing the hydrothermal method: $[Zn_3(BMP)_2L_2(H_2O)_4] \cdot 2H_2O$. The Zn-MOF is a three-dimensional microporous framework and showed strong and stable luminescence in a solid-state and aqueous solution. The luminescence properties of the Zn-MOF in common solvents and aqueous solutions with different pH values were investigated. The application of the Zn-MOF as a sensor in detecting tetracycline and acetone was also explored in this study (Scheme 1).



Scheme 1. The construction and luminescence sensing of the Zn-MOF.

2. Results and Discussion

2.1. The Crystal Structure of $[Zn_3(BMP)_2L_2(H_2O)_4] \cdot 2H_2O$

The Zn-MOF featured a 3D structure, which was crystallized in a monoclinic system with a $P2_1/n$ space group. The asymmetric unit of the Zn-MOF consists of three Zn(II) ions, two L ligands, two BMP ligands, four coordinated water molecules, and two free water molecules. The Zn(II) ions have two different coordination modes. The Zn1 ions had a total of four coordinations: two coordinations with two O atoms from two L ligands and two coordinations with N atoms from BMP ligands, to form a slightly distorted tetrahedron geometry $[Zn1N_2O_2]$ (Figure 1a). The bond length range of Zn1-O is 1.933(2)–1.946(2) Å and the bond length range of Zn1-N is 2.010(3)–2.024(2) Å. The Zn2 ions had six coordinations in the $[Zn2N_2O_4]$ octahedral configuration, which were formed by linking to four O atoms from four water molecules and two nitrogen atoms from two BMP ligands. The Zn2-O bond distances vary from 2.079(2) to 2.118(2) Å and the Zn2-N bond length is 2.140(2) Å. Each BMP is a three-coordination ligand connected with three different Zn(II) ions in $\mu_3:\eta^1\eta^1\eta^1$ coordination mode to form a two-dimensional Zn-BMP network. The L ligand acted as a bridging ligand to link two adjacent Zn1 ions through the $\mu_1:\eta^1\eta^0/\mu_1:\eta^1\eta^0/\mu_0:\eta^0\eta^0$ coordination mode along the a-axis extension, and the Zn-BMP network further formed a three-dimensional structure (Figure 1b). Notably, the three-dimensional framework consisted of two types of helical chains (left-handed and right-handed) having a repeating unit $[Zn1-BMP]$ which consisted of two BMP ligands and two Zn1 ions with a pitch of 15.8197 Å (Figure 1c). $[Zn1-BMP-Zn1-L]$ was composed of a BMP ligand, an L ligand, and two Zn1 ions with a pitch of 15.6548 Å (Figure 1d).

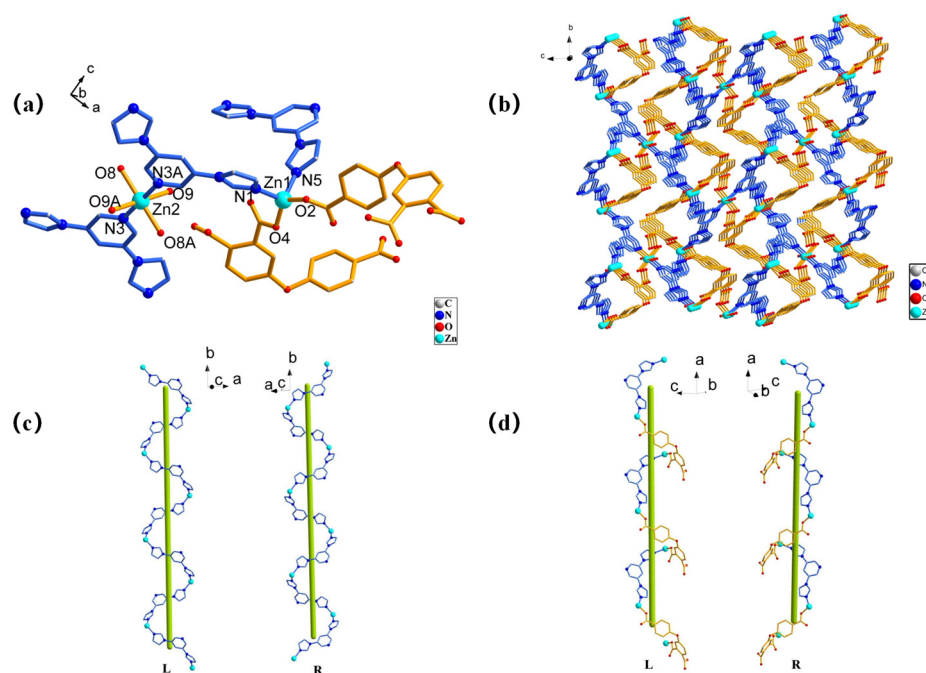


Figure 1. The structure of the Zn-MOF: (a) the coordination environment of Zn ion, (b) the three-dimensional framework, (c) left- and right-handed helix chains of Zn1-BMP, and (d) left- and right-handed helix chains of Zn1-BMP-Zn1-L.

2.2. Morphological Properties and Thermal Stability of the Zn-MOF

The morphology of the Zn-MOF was described using optical microscopy and SEM. The Zn-MOF was colorless and had transparent blocky crystals and featured a 3D structure with a rough surface (Figure S1 in Supplementary Materials). The Zn-MOF's thermal stability was investigated using TGA on samples by raising the temperature from 25 to 800 °C at a rate of 10 °C/min. The TGA data indicated that the Zn-MOF exhibited good thermal stability (Figure S2). As the temperature increased, the complex began to lose weight continuously. The Zn-MOF complex showed a mass loss of 8.12% from 70 °C to 235 °C, which was caused by the loss of free water molecules and coordinated water molecules (calculated value: 8.15%). When the temperature reached 280 °C, a sudden weight loss occurred, and the organic ligands in the Zn-MOF began to decompose. No further weight loss was observed after 510 °C. A total loss of 77.88% was observed until the temperature reached 510 °C when the decomposition of the Zn-MOF was completed (calculated value: 81.55%). The residual weight corresponded to the formation of ZnO.

2.3. The Solid-State Photoluminescence of the Zn-MOF

The solid-state photoluminescence of the H₃L, BMP, and Zn-MOF were examined at room temperature (Figure 2). The spectrum shows that H₃L and BMP ligands exhibited a maximum emission wavelength at 408nm ($\lambda_{\text{ex}} = 358 \text{ nm}$) and 389 nm ($\lambda_{\text{ex}} = 323 \text{ nm}$), respectively, while the Zn-MOF exhibited a broad emission band with a maximum emission wavelength of 385nm ($\lambda_{\text{ex}} = 305 \text{ nm}$), which might be explained by the ligand's $\pi^* \rightarrow \pi$ electron transition.

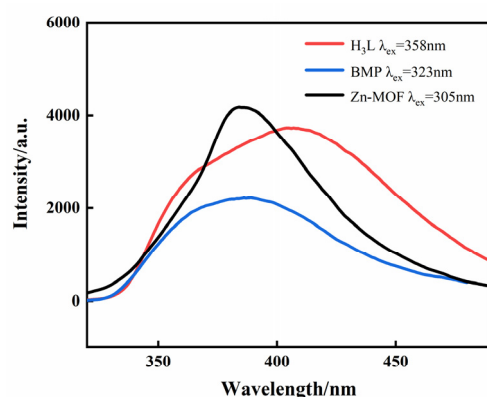


Figure 2. The solid-state emission spectra of the H₃L/BMP ligands and the Zn-MOF.

2.4. Luminescence of the Zn-MOF in Water with Different pH

One of the essential considerations for sensing applications is the stability of MOFs in aquatic environments. The Zn-MOF sample was immersed in water and aqueous solutions with pH of 4, 6, 9, 11, and 12 for 72 h. Comparing the PXRD patterns of the Zn-MOF sample in various aqueous solutions to the pattern obtained for the Zn-MOF crystal, there were no differences (Figure 3a). This verified that the structure of the Zn-MOF was unaltered. This result demonstrated the high chemical stability of the produced Zn-MOF in aqueous solutions over a broad pH range. Meanwhile, Zn-MOF was also the subject of a luminescence experiment in water at pH 1–14. The Zn-MOF powder (3 mg) was dispersed in aqueous solutions (3 mL) with various pH values, and the light-emitting properties were measured. As shown in Figure 3b, under strongly acidic conditions (pH < 3), the H₃L ligand may not have coordinated well with metal Zn²⁺ ions, which resulted in different degrees of a decrease in fluorescence intensity. After the pH value of the solution exceeded 12 (pH > 12), the luminescence intensity of the Zn-MOF diminished sharply. However, at the emission wavelength of 385 nm, the luminescence intensity of the Zn-MOF remained nearly constant for pH values between 4 and 12. In addition, compared with the solid emission spectrum of the Zn-MOF, the emission band in aqueous solution was also observed to have the maximum value at 385 nm with relatively high intensity (Figure S3). This indicated that the prepared Zn-MOF maintained good luminescence properties in water. The stable luminescence properties suggested that the Zn-MOF could be a regular and potentially helpful material as a luminescent sensor in aqueous solutions.

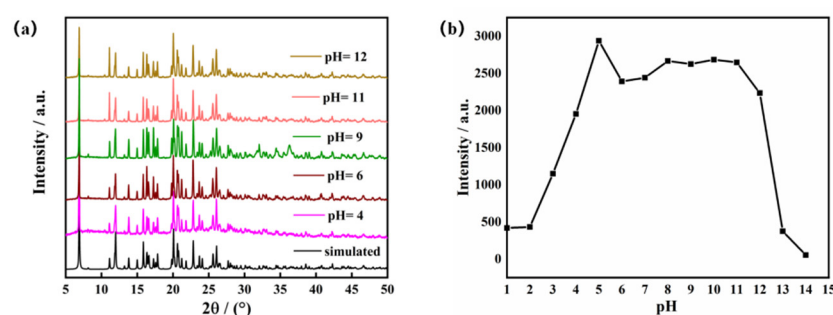


Figure 3. (a) The PXRD patterns of the Zn-MOF, and (b) the luminescence intensity of the Zn-MOF in different pH aqueous solutions.

2.5. The Luminescence Properties of the Zn-MOF in Solvents and Sensing for Acetone

The luminescence of the Zn-MOF was investigated in the presence of common organic solvents to explore the stability of the Zn-MOF in a solvent environment. The Zn-MOF (3 mg) was dispersed in 3 mL of common solvents (water, acetone, dichloromethane, methanol, ethanol, DMA, DMF, DMSO, acetonitrile, etc.) to form suspensions. The luminescence spectra of these suspensions were obtained at an excitation of 305 nm. As shown

in Figure 4, the Zn-MOF showed excellent luminescence performance in some commonly used organic solvents. However, it is worth noting that the luminescence of the Zn-MOF in acetone nearly disappeared, suggesting that the Zn-MOF can be used as a luminescent sensor to detect acetone molecules.

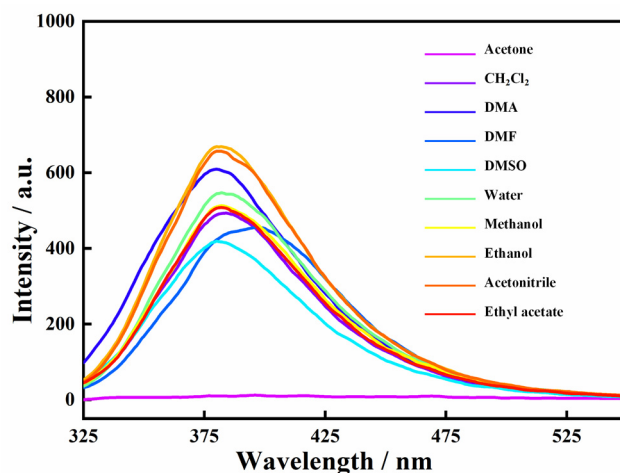


Figure 4. Luminescence emission spectra of the Zn-MOF in different solvents.

To further explore the influence of the acetone molecule on the luminescence intensity of the Zn-MOF, acetone solution was added to the suspension to perform luminescence titration experiments. Acetone solution in the quantity of 10 μL was added dropwise to a beaker containing a 3 mg sample, and the luminescence intensity of the system at 385 nm was monitored. As shown in Figure 5, when the volume of the acetone solution increased from 0 μL to 300 μL , the luminescence intensity of the Zn-MOF gradually decreased. When 300 μL of acetone solution was added, the luminescence quenching efficiency (QE) of the Zn-MOF was observed to be 67%. The luminescence intensity of the Zn-MOF had a specific linear relationship with the volume fraction of acetone added as per the following linear equation: $I_0/I - 1 = K_{SV}V$.

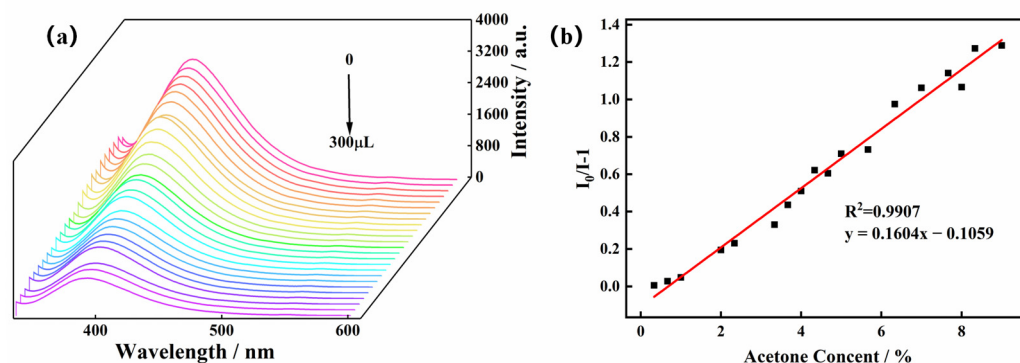


Figure 5. (a) Emission spectra of the Zn-MOF with the addition of acetone and (b) the SV plot for the quenching effect of acetone on the luminescence of the Zn-MOF under 305 nm.

Here, I_0 and I are the luminescence intensity before and after adding acetone, respectively; V is the volume fraction of acetone in water; and K_{SV} is the slope of the linear equation [9]. The correlation coefficient (R^2) was found to be 0.9907. The limit of detection (LOD) of the Zn-MOF for acetone was calculated as 0.1597%, indicating that the Zn-MOF can detect acetone molecules in a low concentration range.

To explore the selective detection of the Zn-MOF for the acetone molecule, the Zn-MOF sample (3 mg) was immersed in different organic solvents (ethyl acetate, ethanol, methanol, methyl ethyl ketone, dichloromethane, etc.). An equal amount of acetone was then added for the anti-interference experiment. As shown in Figure S4, it was found that

only the presence of acetone molecules in organic solvents weakened the luminescence of the Zn-MOF, and the quenching effect of acetone on the luminescence of the Zn-MOF was not affected by the interfering solvents.

2.6. Luminescence Sensing of the Zn-MOF to TC

Residual TC has been identified as a major organic contaminant in water. Being present in aquatic ecosystems, this non-degradable contaminant is harmful to the environment and human health. Therefore, the creation of reliable and efficient techniques to identify TC pollutants in water is urgently needed. So, the luminescence sensing of the Zn-MOF to TC was investigated. The Zn-MOF samples (3 mg) were soaked in different antibiotics (1×10^{-3} mol/L, 3 mL), such as penicillin (PEN), chloramphenicol (THI), griseofulvin (GRI), erythromycin (ERY), streptomycin (STR), and kanamycin (KANA). The solutions were then subjected to ultrasound treatment for 30 min to obtain a uniform suspension. Figure 6a shows that TC weakened the luminescence of the Zn-MOF when different antibiotics were added to the suspension of the Zn-MOF. Moreover, upon introducing TC to the mixture of the Zn-MOF and the alternative antibiotic, the luminescent emission of the Zn-MOF was significantly quenched (Figure 6b). Therefore, the prepared Zn-MOF showed good selectivity and sensitivity to the detection of TC in the presence of other antibiotics.

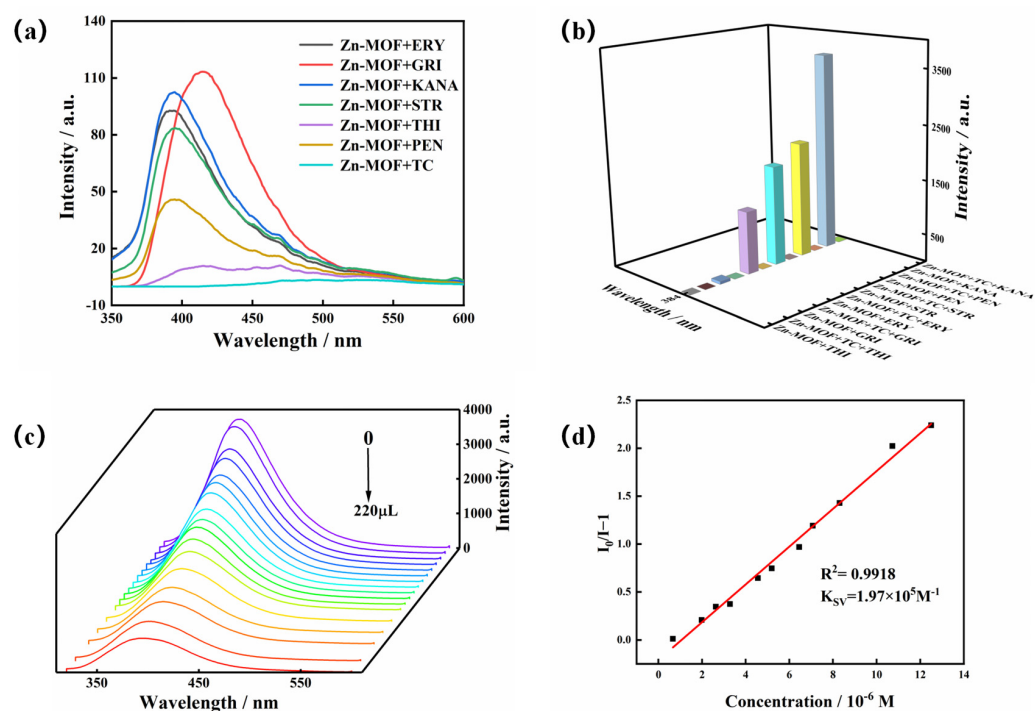


Figure 6. (a) Emission spectra of the Zn-MOF in the presence of different antibiotics, (b) luminescence intensity of the Zn-MOF in the presence of other interfering antibiotics with TC and without TC, (c) emission spectra of the Zn-MOF with the addition of TC, and (d) the SV plot for the quenching effect of TC on the luminescence of the Zn-MOF ($\lambda_{ex} = 305$ nm).

To explore the effect of TC on the luminescence intensity of the Zn-MOF, a luminescence titration experiment was performed by gradually adding TC to a suspension of the Zn-MOF and monitoring the emission intensity at 385 nm (Figure 6c). When the volume of TC solution (2×10^{-4} mol/L) was increased from 0 to 220 μ L, the emission intensity of the Zn-MOF gradually decreased. A good linear relationship between luminescence intensity and TC concentration was visible at low concentrations (Figure 6d). The calculated KSV was $1.97 \times 10^5 M^{-1}$, and the R^2 was 0.9918. In addition, the LOD for TC was estimated to be 3.34 μ M. In addition, taking pH = 4 or 10 as an example, the fluorescence sensing ability of the Zn-MOF to TC in acidic and alkaline conditions was also tested. The LOD of TC in slightly

acidic and alkaline aqueous solutions (pH = 4 and 10) was calculated using fluorescence titration and was found to be 5.17 μM and 7.27 μM , respectively (Figure 7). It indicated that the Zn-MOF had the ability to detect TC in the aqueous system of pH 4–10. These results demonstrated the high selectivity and anti-interference capability of the prepared Zn-MOF for TC detection.

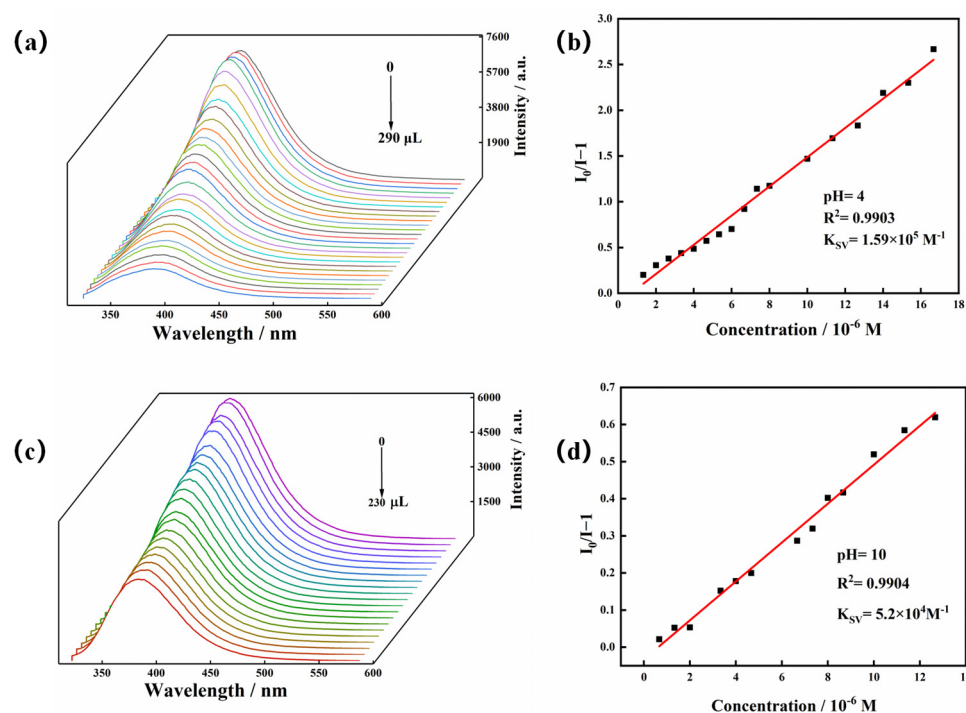


Figure 7. (a) Emission spectra of the Zn-MOF with the addition of TC (pH = 4), (b) the SV plot for the quenching effect of TC on the luminescence of the Zn-MOF (pH = 4), (c) emission spectra of the Zn-MOF with the addition of TC (pH = 10), and (d) the SV plot for the quenching effect of TC on the luminescence of the Zn-MOF (pH = 10).

The most crucial aspects when evaluating a sensor material for practical applications are response time and recyclability. Measurements of the time-dependent luminescence were carried out to confirm the response rate of the Zn-MOF. The emission of the Zn-MOF was immediately quenched by exposure to TC for 10.11s (Figure S5a), indicating rapid detection of TC with the luminescence of the Zn-MOF. Moreover, the recovery performance of the Zn-MOF as a TC luminescent sensor was evaluated to fulfil the recyclability requirements for potential practical applications. Therefore, a recycling experiment was conducted to assess the recycling and regeneration capabilities of the Zn-MOF. Firstly, the suspension containing TC was centrifuged and dried to recover the Zn-MOF powder, which was then washed with ethanol to remove the TC. The luminescence of the Zn-MOF was recorded. The experimental results showed that the luminescence intensity of the Zn-MOF was not affected much after four recycling cycles (Figure S5b). This indicated that Zn-MOF could be reused for sample detection after simple solvent washing.

2.7. Luminescence Sensing of the Zn-MOF for TC in Urine and Aquaculture Wastewater Systems

Antibiotics in urine have become an important biomarker for studying human exposure to antibiotics. Therefore, the presence of TC was detected in human urine using the prepared Zn-MOF. The Zn-MOF was immersed in the urine with TC and without TC for three days, which also included some interfering agents (NaCl, hippuric acid, creatinine, glucose, urea, L-cysteine, etc.). The results of the experiments are shown in Figure 8a. It was found that only the presence of TC in urine quenches the luminescence of the Zn-MOF, and the quenching effect of TC on the luminescence of the Zn-MOF was not affected by the interfering agents, confirming that the Zn-MOF has high selectivity for sensing TC.

Elevated levels of TC in water bodies due to the large-scale use of tetracycline antibiotics in the pharmaceutical and aquaculture industries pose an increased ecological risk to the environment. Therefore, it is necessary to detect TC in aquaculture wastewater plants. TC was added to a suspension of the Zn-MOF containing some inorganic material and additional antibiotics (sulfadiazine (SDZ) and sulfamethazine (SMZ)). It was found that only the presence of TC in aquaculture wastewater quenches the luminescence of the Zn-MOF, and the quenching effect of TC on the luminescence of the Zn-MOF was not affected by the interfering agents (Figure 8b). It was observed that the Zn-MOF had high selectivity for the detection of TC. These findings suggest that the prepared Zn-MOF has the potential to detect TC for practical applications.

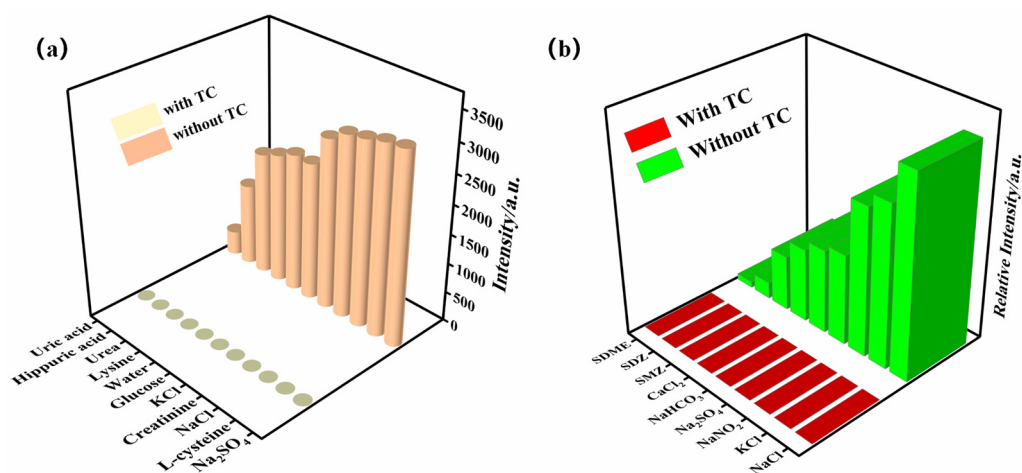


Figure 8. Luminescence intensity of the Zn-MOF in urine (a) and in the aquaculture wastewater system (b).

2.8. The Luminescence Sensing Mechanism

The luminescence sensing mechanism of the Zn-MOF was investigated. Firstly, the PXRD pattern of the Zn-MOF immersed in TC and acetone solution for 48 h was obtained. It can be seen from Figure 9a that the peak positions and intensities of the spectra, before and after the detection of TC and acetone solutions, remained unchanged. This indicates that the structure of the Zn-MOF remained intact after the luminescence experiment. This implies that the prepared Zn-MOF was stable in TC and acetone solutions, and the luminescence quenching of the Zn-MOF by TC and acetone cannot be attributed to the collapse of the framework.

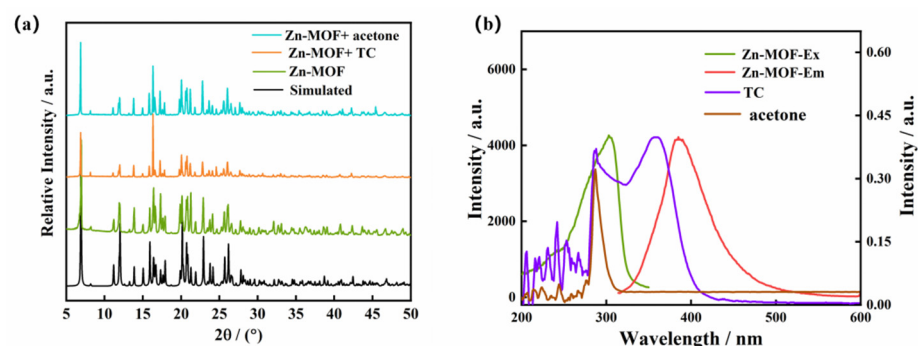


Figure 9. (a) PXRD pattern of the Zn-MOF after luminescence sensing of TC and acetone, and (b) excitation and emission spectra of the Zn-MOF and UV absorption spectra of TC and acetone.

The targeted substrates for detection, TC, and acetone were studied using UV-Vis absorption. Figure 9b shows that TC had a broad absorption band in the range of 300–400 nm and acetone had a strong absorption band in the field of 200–300 nm. The Zn-MOF was

observed to have a strong emission band at 385 nm and an excitation band at 305 nm. Therefore, the UV absorption spectra of TC and acetone overlapped with the excitation spectra of the Zn-MOF complex, indicating that the luminescence quenching of the Zn-MOF by TC and acetone was caused by the fluorescence resonance energy transfer (FRET). This suggests that the absorption of incident light by TC and acetone was competitive with that of the prepared Zn-MOF [47,48].

Similarly, photoinduced electron transfer (PET) was also considered as a possible luminescence quenching mechanism. DFT calculations were also performed to investigate the detection mechanism of the Zn-MOF for TC and acetone (Figure 10). According to DFT, the LUMO of H₃L (−1.17 eV) and the LUMO of BMP (−1.96 eV) were higher than the LUMO of TC (−2.31 eV) but lower than that of acetone (−0.37 eV). Since the LUMO level of the TC was in a lower energy state, the properties of H₃L and BMP ligands mentioned above enabled the transfer of excited electrons from the framework of the Zn-MOF to TC (LUMO energy from −1.17 eV to −2.31 eV). Therefore, according to these findings, both FRET and PET processes can be considered as the reasonable quenching mechanisms.

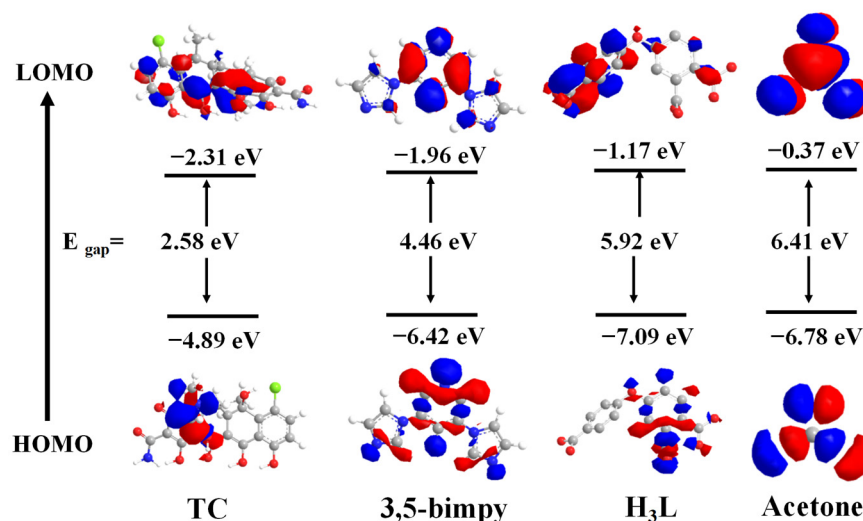


Figure 10. HOMO and LUMO of ligands BMP, H₃L, acetone, and TC.

3. Materials and Methods

3.1. Materials

Every reagent was bought from a store and utilized straight away. Using an elemental Vario EL analyzer, elemental analyses (C, H, and N) were performed. The KBr pellet method was used to record infrared (IR) spectra using a Bruker Tensor37 spectrophotometer. On a PANalytical X'pert PRO MPD diffractometer using CuK α radiation ($\lambda = 1.5406 \text{ \AA}$), experimental powder X-ray diffraction (PXRD) was performed. Using a nitrogen environment and a heating rate of min^{-1} from room temperature to $800 \text{ }^\circ\text{C}$, thermogravimetric analysis (TGA) was performed using an HCT-2 thermal analyzer. An FL7000 fluorescence spectrophotometer was used to record the solid and liquid fluorescence spectra at room temperature. Using a U-3900H spectrophotometer, UV-Vis spectroscopy was carried out.

3.2. Synthesis of the Zn-MOF

A 25 mL Teflon cup containing Zn(Ac)₂ (0.2 mmol), H₃L (0.1 mmol), BMP (0.2 mmol), NaOH (0.4 mL, $1 \text{ mol}\cdot\text{L}^{-1}$), and water (10 mL) was heated at $120 \text{ }^\circ\text{C}$ for 72 h, then cooled to room temperature. For C₅₂, H₄₄, Zn₃ N₁₀ O₂₀, elemental analysis (%) C, 47.09; N, 10.57; H, 3.32; found (%) C, 47.12; N, 10.61; H, 3.34. IR(KBr pellet, cm^{-1}), 3590 (w), 3449 (w), 3246 (m), 3131 (s), 1612 (s), 1562 (m), 1522 (m), 1379 (s), 1314 (w), 1256 (m), 1235 (s), 1155 (m), 1075 (s), 1012 (s), 964 (w), 948 (s), 847 (m), 814 (w), 789(w), 764 (s), 737 (s), 691 (m), 648 (m), 517 (w), 452 (w). The CCDC Number of Zn-MOF was detailed in the Appendix A.

3.3. X-ray Crystallographic Study

The Cu K α ($\lambda = 0.154184$ nm) was used in an X-ray diffractometer to gather the crystal data. The SHELXL 97 and SHELXL 97 programs were used to solve the structure. The coordinates of the hydrogen atoms were established using the theoretical hydrogenation approach and were then adjusted using the full-matrix least-squares method. The crystallographic data are summarized in Table S1, and the selected bond lengths and angles are presented in Table S2.

3.4. Luminescence Measurements

The Zn-MOF powder sample (3 mg) was added to deionized water (3 mL); then, the solution was ultrasonicated for 30 min to form a uniform suspension. The suspension was added to a quartz cuvette. The luminescence emission spectra were recorded at the excitation of 305 nm after each incremental addition of 10 μ L TC solution (2×10^{-4} mol/L) at room temperature.

The quenching constant was calculated using the Stern-Volmer (SV) equation:

$I_0/I - 1 = K_{SV} [A]$. Here, K_{SV} is the quenching constant; $[A]$ is the molar concentration of TC; and I_0 and I are the luminescence before and after TC addition strength.

The LOD of the Zn-MOF for TC can be determined as follows:

$LOD = 3\sigma/K_{SV}$. Here, LOD is the limit of detection, and σ is the standard deviation of the three repeated luminescence measurements of the Zn-MOF in a blank aqueous solution.

4. Conclusions

A new Zn-MOF, $[Zn_3(BMP)_2L_2(H_2O)_4] \cdot 2H_2O$, was designed and synthesized using BMP and H₃L ligands. The synthesized Zn-MOF had a three-dimensional framework in which the BMP ligand adopted the $\mu_3:\eta^1\eta^1\eta^1$ coordination mode, while the L ligand adopted the $\mu_1:\eta^1\eta^0/\mu_1:\eta^1\eta^0/\mu_0:\eta^0\eta^0$ coordination mode. The Zn-MOF exhibited excellent luminescence in solids and solutions, and the luminescence properties remained stable at pH values ranging from 4 to 10. The Zn-MOF fabricated in this study can be used as a luminescent sensor to detect acetone and TC in water. The detection limits of the Zn-MOF were found to be 3.34 μ M and 0.1597% for TC and acetone, respectively. TC could be detected by the Zn-MOF in urine and aquaculture wastewater systems. The luminescence quenching mechanisms of the Zn-MOF were investigated in detail using experimental methods and theoretical calculations. These findings suggest that the Zn-MOF is an excellent luminescent material that can be used for detecting environmental pollutants such as TC and acetone.

Supplementary Materials: The following supporting information can be downloaded at <https://www.mdpi.com/article/10.3390/molecules28030999/s1>: Figure S1: (a) Optical microscopy image and (b) SEM image of the Zn-MOF; Figure S2: TGA curve of the Zn-MOF; Figure S2: The emission spectra of the Zn-MOF in solids and water; Figure S3: The luminescence intensity of the Zn-MOF in different interfering solvents with and without acetone; Figure S4: (a) Time response of the Zn-MOF to TC and (b) recycling experiment; Figure S5; Table S1: The crystal data of the Zn-MOF; Table S2: Selected bond lengths [\AA] and angles [$^\circ$] for the Zn-MOF.

Author Contributions: Conceptualization, N.W.; methodology, N.W. and S.L.; software, Y.G.; validation, Z.L. and S.L.; formal analysis, N.W. and Z.L.; investigation, S.L.; resources, X.L.; data curation, N.W. and Z.L.; writing—original draft preparation, N.W. and Z.L.; writing—review and editing, X.L.; visualization, Y.G.; supervision, X.L.; funding acquisition, X.L. All authors have read and agreed to the published version of the manuscript.

Funding: This research was funded by the key project of science and technology plan of Beijing Education Commission (KZ201910028038) and the National Natural Science Foundation of China (21471104).

Institutional Review Board Statement: Not applicable.

Informed Consent Statement: Not applicable.

Data Availability Statement: Not applicable.

Acknowledgments: This research was financially supported by the key project of science and technology plan of Beijing Education Commission (KZ201910028038) and the National Natural Science Foundation of China (21471104).

Conflicts of Interest: The authors declare no conflict of interest.

Sample Availability: Samples of the compounds are available from the authors.

Appendix A

CCDC 2167668 contains the supplementary crystallographic data for this paper. The data can be obtained free of charge via www.ccdc.cam.ac.uk/structures/ (accessed on 14 January 2023), or by emailing data_request@ccdc.cam.ac.uk.

References

1. Safaei, M.; Foroughi, M.M.; Ebrahimpoor, N.; Jahani, S.; Omid, A.; Khatami, M. A review on metal-organic frameworks: Synthesis and applications. *TrAC Trends Anal. Chem.* **2019**, *118*, 401–425. [CrossRef]
2. Pettinari, C.; Pettinari, R.; Di Nicola, C.; Tombesi, A.; Scuri, S.; Marchetti, F. Antimicrobial MOFs. *Coord. Chem. Rev.* **2021**, *446*, 214121. [CrossRef]
3. Zhang, L.; Sun, Y.; Zhang, Z.; Shen, Y.; Li, Y.; Ma, T.; Zhang, Q.; Ying, Y.; Fu, Y. Portable and durable sensor based on porous MOFs hybrid sponge for fluorescent-visual detection of organophosphorus pesticide. *Biosens Bioelectron.* **2022**, *216*, 114659. [CrossRef]
4. Liu, L.; Chen, Q.; Lv, J.; Li, Y.; Wang, K.; Li, J.R. Stable Metal-Organic Frameworks for Fluorescent Detection of Tetracycline Antibiotics. *Inorg. Chem.* **2022**, *61*, 8015–8021. [CrossRef] [PubMed]
5. Xu, J.; Guo, S.; Jia, L.; Zhu, T.; Chen, X.; Zhao, T. A smartphone-integrated method for visual detection of tetracycline. *Chem. Eng. J.* **2021**, *416*, 127741. [CrossRef]
6. Li, K.; Li, J.J.; Zhao, N.; Ma, Y.; Di, B. Removal of Tetracycline in Sewage and Dairy Products with High-Stable MOF. *Molecules* **2020**, *25*, 1312. [CrossRef]
7. Lyu, L.; Xie, Q.; Yang, Y.; Wang, R.; Cen, W.; Luo, S.; Yang, W.; Gao, Y.; Xiao, Q.; Zou, P.; et al. A novel CeO₂ Hollow-Shell sensor constructed for high sensitivity of acetone gas detection. *Appl. Surf. Sci.* **2022**, *571*, 151337. [CrossRef]
8. Joshi, S.; Tonde, S.; Wakhure, U.; Bornare, D.; Chatterjee, A.; Syed, K.; Sunkara, M.V. Hierarchical CaTiO₃ microspheres for acetone sensing. *Sens. Actuators B Chem.* **2022**, *359*, 131621. [CrossRef]
9. Li, Y.; Song, H.; Chen, Q.; Liu, K.; Zhao, F.-Y.; Ruan, W.-J.; Chang, Z. Two coordination polymers with enhanced ligand-centered luminescence and assembly imparted sensing ability for acetone. *J. Mater. Chem. A* **2014**, *2*, 9469–9473. [CrossRef]
10. Xu, H.; Mi, H.Y.; Guan, M.M.; Shan, H.Y.; Fei, Q.; Huan, Y.F.; Zhang, Z.Q.; Feng, G.D. Residue analysis of tetracyclines in milk by HPLC coupled with hollow fiber membranes-based dynamic liquid-liquid micro-extraction. *Food Chem.* **2017**, *232*, 198–202. [CrossRef]
11. Bu, T.; Jia, P.; Sun, X.; Liu, Y.; Wang, Q.; Wang, L. Hierarchical molybdenum disulfide nanosheets based lateral flow immunoassay for highly sensitive detection of tetracycline in food samples. *Sens. Actuators B Chem.* **2020**, *320*, 128440. [CrossRef]
12. Deng, B.; Xu, Q.; Lu, H.; Ye, L.; Wang, Y. Pharmacokinetics and residues of tetracycline in crucian carp muscle using capillary electrophoresis on-line coupled with electrochemiluminescence detection. *Food Chem.* **2012**, *134*, 2350–2354. [CrossRef] [PubMed]
13. Wang, G.; Liu, H.; Wang, J.; Gong, P.; Cai, C.; Dai, X.; Wang, P. Pretreatment of spiramycin fermentation residue by thermally activated peroxydisulfate for improving biodegradability: Insights into matrix disintegration and antibiotics degradation. *Chemical. Eng. J.* **2022**, *427*, 130973. [CrossRef]
14. Abazari, R.; Mahjoub, A.R.; Shariati, J. Synthesis of a nanostructured pillar MOF with high adsorption capacity towards antibiotics pollutants from aqueous solution. *J. Hazard. Mater.* **2019**, *366*, 439–451. [CrossRef]
15. Cui, Y.; Zhang, J.; He, H.; Qian, G. Photonic functional metal-organic frameworks. *Chem. Soc. Rev.* **2018**, *47*, 5740–5785. [CrossRef] [PubMed]
16. Zhou, Y.; Yang, Q.; Zhang, D.; Gan, N.; Li, Q.; Cuan, J. Detection and removal of antibiotic tetracycline in water with a highly stable luminescent MOF. *Sens. Actuators B: Chem.* **2018**, *262*, 137–143. [CrossRef]
17. Chen, Y.; Yang, Y.; Orr, A.A.; Makam, P.; Redko, B.; Haimov, E.; Wang, Y.; Shimon, L.J.W.; Rencus-Lazar, S.; Ju, M.; et al. Self-Assembled Peptide Nano-Superstructure towards Enzyme Mimicking Hydrolysis. *Angew. Chem. Int. Ed. Engl.* **2021**, *60*, 17164–17170. [CrossRef]
18. Chen, Y.; Guerin, S.; Yuan, H.; O'Donnell, J.; Xue, B.; Cazade, P.A.; Haq, E.U.; Shimon, L.J.W.; Rencus-Lazar, S.; Tofail, S.A.M.; et al. Guest Molecule-Mediated Energy Harvesting in a Conformationally Sensitive Peptide-Metal Organic Framework. *J. Am. Chem. Soc.* **2022**, *144*, 3468–3476. [CrossRef]
19. Zhao, D.; Yu, S.; Jiang, W.J.; Cai, Z.H.; Li, D.L.; Liu, Y.L.; Chen, Z.Z. Recent Progress in Metal-Organic Framework Based Fluorescent Sensors for Hazardous Materials Detection. *Molecules* **2022**, *27*, 2226. [CrossRef]
20. Li, P.Z.; Wang, X.J.; Liu, J.; Lim, J.S.; Zou, R.; Zhao, Y. A Triazole-Containing Metal-Organic Framework as a Highly Effective and Substrate Size-Dependent Catalyst for CO₂ Conversion. *J. Am. Chem. Soc.* **2016**, *138*, 2142–2145. [CrossRef]

21. Shah, M.S.; Tsapatsis, M.; Siepmann, J.I. Hydrogen Sulfide Capture: From Absorption in Polar Liquids to Oxide, Zeolite, and Metal-Organic Framework Adsorbents and Membranes. *Chem. Rev.* **2017**, *117*, 9755–9803. [[CrossRef](#)] [[PubMed](#)]
22. Liu, J.; Chen, L.; Cui, H.; Zhang, J.; Zhang, L.; Su, C.Y. Applications of metal-organic frameworks in heterogeneous supramolecular catalysis. *Chem. Soc. Rev.* **2014**, *43*, 6011–6061. [[CrossRef](#)] [[PubMed](#)]
23. Huang, Y.; Lin, Z.; Cao, R. Palladium nanoparticles encapsulated in a metal-organic framework as efficient heterogeneous catalysts for direct C2 arylation of indoles. *Chemistry* **2011**, *17*, 12706–12712. [[CrossRef](#)] [[PubMed](#)]
24. Chen, J.; Cheng, F.; Luo, D.; Huang, J.; Ouyang, J.; Nezamzadeh-Ejehieh, A.; Khan, M.S.; Liu, J.; Peng, Y. Recent advances in Ti-based MOFs in biomedical applications. *Dalton. Trans.* **2022**, *51*, 14817–14832. [[CrossRef](#)] [[PubMed](#)]
25. Minguez Espallargas, G.; Coronado, E. Magnetic functionalities in MOFs: From the framework to the pore. *Chem. Soc. Rev.* **2018**, *47*, 533–557. [[CrossRef](#)]
26. Coronado, E.; Minguez Espallargas, G. Dynamic magnetic MOFs. *Chem. Soc. Rev.* **2013**, *42*, 1525–1539. [[CrossRef](#)]
27. Wang, H.; Liu, D.; Wei, M.; Qi, W.; Li, X.; Niu, Y. A stable and highly luminescent 3D Eu(III)-organic framework for the detection of colchicine in aqueous environment. *Environ. Res.* **2022**, *208*, 112652. [[CrossRef](#)]
28. Liu, D.; Dong, G.; Wang, X.; Nie, F.; Li, X. A luminescent Eu coordination polymer with near-visible excitation for sensing and its homologues constructed from 1,4-benzenedicarboxylate and 1H-imidazo[4,5-f][1,10]-phenanthroline. *CrystEngComm* **2020**, *22*, 7877–7887. [[CrossRef](#)]
29. Allendorf, M.D.; Bauer, C.A.; Bhakta, R.K.; Houk, R.J. Luminescent metal-organic frameworks. *Chem. Soc. Rev.* **2009**, *38*, 1330–1352. [[CrossRef](#)]
30. Wang, B.; Lv, X.L.; Feng, D.; Xie, L.H.; Zhang, J.; Li, M.; Xie, Y.; Li, J.R.; Zhou, H.C. Highly Stable Zr(IV)-Based Metal-Organic Frameworks for the Detection and Removal of Antibiotics and Organic Explosives in Water. *J. Am. Chem. Soc.* **2016**, *138*, 6204–6216. [[CrossRef](#)]
31. Wang, B.; Yang, Q.; Guo, C.; Sun, Y.; Xie, L.H.; Li, J.R. Stable Zr(IV)-Based Metal-Organic Frameworks with Predesigned Functionalized Ligands for Highly Selective Detection of Fe(III) Ions in Water. *ACS Appl. Mater. Interfaces* **2017**, *9*, 10286–10295. [[CrossRef](#)] [[PubMed](#)]
32. Yang, J.; Che, J.; Jiang, X.; Fan, Y.; Gao, D.; Bi, J.; Ning, Z. A Novel Turn-On Fluorescence Probe Based on Cu(II) Functionalized Metal-Organic Frameworks for Visual Detection of Uric Acid. *Molecules* **2022**, *27*, 4803. [[CrossRef](#)] [[PubMed](#)]
33. Kirchon, A.; Feng, L.; Drake, H.F.; Joseph, E.A.; Zhou, H.C. From fundamentals to applications: A toolbox for robust and multifunctional MOF materials. *Chem. Soc. Rev.* **2018**, *47*, 8611–8638. [[CrossRef](#)]
34. Ahmadijokani, F.; Molavi, H.; Rezakazemi, M.; Aminabhavi, T.M.; Arjmand, M. Simultaneous detection and removal of fluoride from water using smart metal-organic framework-based adsorbents. *Coord. Chem. Rev.* **2021**, *445*, 214037. [[CrossRef](#)]
35. Huang, D.; Wang, Y.; Wang, X.; Li, H.; Tan, X.; Chen, Y.; Wang, W.; Cheng, Q.; Yi, M.; Han, G.; et al. Rational in situ construction of Fe-modified MXene-derived MOFs as high-performance acetone sensor. *Chem. Eng. J.* **2022**, *444*, 136526. [[CrossRef](#)]
36. Gan, Z.; Hu, X.; Xu, X.; Zhang, W.; Zou, X.; Shi, J.; Zheng, K.; Arslan, M. A portable test strip based on fluorescent europium-based metal-organic framework for rapid and visual detection of tetracycline in food samples. *Food Chem.* **2021**, *354*, 129501. [[CrossRef](#)] [[PubMed](#)]
37. Zhu, X.D.; Zhang, K.; Wang, Y.; Long, W.W.; Sa, R.J.; Liu, T.F.; Lu, J. Fluorescent Metal-Organic Framework (MOF) as a Highly Sensitive and Quickly Responsive Chemical Sensor for the Detection of Antibiotics in Simulated Wastewater. *Inorg. Chem.* **2018**, *57*, 1060–1065. [[CrossRef](#)]
38. Gai, S.; Zhang, J.; Fan, R.; Xing, K.; Chen, W.; Zhu, K.; Zheng, X.; Wang, P.; Fang, X.; Yang, Y. Highly Stable Zinc-Based Metal-Organic Frameworks and Corresponding Flexible Composites for Removal and Detection of Antibiotics in Water. *ACS Appl. Mater. Interfaces* **2020**, *12*, 8650–8662. [[CrossRef](#)]
39. Pramanik, S.; Zheng, C.; Zhang, X.; Emge, T.J.; Li, J. New microporous metal-organic framework demonstrating unique selectivity for detection of high explosives and aromatic compounds. *J. Am. Chem. Soc.* **2011**, *133*, 4153–4155. [[CrossRef](#)]
40. Xian, G.; Wang, L.; Wan, X.; Yan, H.; Cheng, J.; Chen, Y.; Lu, J.; Li, Y.; Li, D.; Dou, J.; et al. Two Multiresponsive Luminescent Zn-MOFs for the Detection of Different Chemicals in Simulated Urine and Antibiotics/Cations/Anions in Aqueous Media. *Inorg. Chem.* **2022**, *61*, 7238–7250. [[CrossRef](#)]
41. Mandal, A.; Adhikary, A.; Sarkar, A.; Das, D. Naked Eye Cd(2+) Ion Detection and Reversible Iodine Uptake by a Three-Dimensional Pillared-Layered Zn-MOF. *Inorg. Chem.* **2020**, *59*, 17758–17765. [[CrossRef](#)] [[PubMed](#)]
42. Zhang, D.S.; Gao, Q.; Chang, Z.; Liu, X.T.; Zhao, B.; Xuan, Z.H.; Hu, T.L.; Zhang, Y.H.; Zhu, J.; Bu, X.H. Rational Construction of Highly Tunable Donor-Acceptor Materials Based on a Crystalline Host-Guest Platform. *Adv. Mater.* **2018**, *30*, e1804715. [[CrossRef](#)] [[PubMed](#)]
43. Zhang, S.-Q.; Jiang, F.-L.; Wu, M.-Y.; Ma, J.; Bu, Y.; Hong, M.-C. Assembly of Discrete One-, Two-, and Three-Dimensional Zn(II) Complexes Containing Semirigid V-Shaped Tricarboxylate Ligands. *Cryst. Growth Des.* **2012**, *12*, 1452–1463. [[CrossRef](#)]
44. Zhang, S.-Q.; Jiang, F.-L.; Bu, Y.; Wu, M.-Y.; Ma, J.; Shan, X.-C.; Xiong, K.-C.; Hong, M.-C. Two dual-emissive Zn(ii) coordination polymers with tunable photoluminescence properties. *CrystEngComm* **2012**, *14*, 6394–6396. [[CrossRef](#)]
45. Wang, Z.; Zhao, L.; Han, Y.; Song, G.; Jing, H.; Guo, G.; Wang, Z.; Li, J. Metal-organic frameworks constructed from tetradentate carboxylic acids: Structural diversity, Fluorescence (Fe³⁺ detection) and Dye adsorption properties. *J. Mol. Struct.* **2022**, *1270*, 133925. [[CrossRef](#)]

46. Yuan, F.; Yuan, C.-M.; Zhou, C.-S.; Qiao, C.-F.; Lu, L.; Ma, A.-Q.; Singh, A.; Kumar, A. Syntheses and photocatalytic properties of three new d10-based coordination polymers: Effects of metal centres and ancillary ligands. *CrystEngComm* **2019**, *21*, 6558–6565. [[CrossRef](#)]
47. Yi, K.; Zhang, L. Designed Eu(III)-functionalized nanoscale MOF probe based on fluorescence resonance energy transfer for the reversible sensing of trace Malachite green. *Food Chem.* **2021**, *354*, 129584. [[CrossRef](#)]
48. Wang, J.X.; Yin, J.; Shekhah, O.; Bakr, O.M.; Eddaoudi, M.; Mohammed, O.F. Energy Transfer in Metal-Organic Frameworks for Fluorescence Sensing. *ACS Appl. Mater. Interfaces* **2022**, *14*, 9970–9986. [[CrossRef](#)]

Disclaimer/Publisher’s Note: The statements, opinions and data contained in all publications are solely those of the individual author(s) and contributor(s) and not of MDPI and/or the editor(s). MDPI and/or the editor(s) disclaim responsibility for any injury to people or property resulting from any ideas, methods, instructions or products referred to in the content.